IEEE Journal of Microwaves

Received 3 May 2025; revised 9 July 2025; accepted 7 August 2025.

Digital Object Identifier 10.1109/JMW.2025.3598986

Direct Least-Squares Rational-Polynomial Lumped-Circuit Model Extraction and Group Theory

JAMES C. RAUTIO (Life Fellow, IEEE)

(Regular Paper)

Sonnet Software, Syracuse, NY 13203 USA

(e-mail: rautio@ieee.org)

ABSTRACT Given a measured frequency domain response, it is useful to determine the best fit rational polynomial transfer function and then synthesize a corresponding lumped network. Vector Fitting, an iterative algorithm, is often used for this purpose. Historically, certain avenues of vector fitting research have not been pursued due to numerical precision limitations. Here, we explore one such approach that is closed form, i.e., non-iterative, and is not limited by numerical precision. When a lumped model is desired, we synthesize the best fits of all networks possible that have up to five RLC elements. In the course of this work, a variety of previously unknown relationships between these networks was discovered, including 4651 transforms between these lumped networks. The entire library, closed-form model extraction, and all network-pair transforms have been implemented in MATLAB and is freely available. In conjunction with this work, RLC network transfer functions and networks are explored in terms of group theory.

INDEX TERMS Least-squares, group theory, lumped model, model extraction, networks, rational polynomial, reduced-order models, vector fitting.

I. INTRODUCTION

Given a measured frequency response of a circuit, our objectives are to 1) Extract an accurate rational polynomial model, and 2) Determine one or more compact lumped circuits that correspond to that rational polynomial. There has been extensive work over the last two decades addressing these problems, much of it in terms of the Vector Fitting technique, [1], [2], with a detailed overview of the current state-of-the-art in [3]. This widely used technique is iterative and relies on a reasonable initial selection of transfer function poles. While lumped circuit models appropriate for simulation can be easily found, those models rarely correspond physically to the structure being modeled, limiting physical insight.

A closed form extraction that can yield a physical model for individual discontinuities was described in [4]. However, while the technique requires very few data points, it cannot tolerate noise in the data. Thus, it can be applied only to noise-free data, for example, that generated by a high accuracy EM analysis.

In this paper, I first review the relative advantages and disadvantages of several error metrics that may be minimized to realize a rational polynomial that best fits noisy data in a least-squares sense. I then investigate applying one of those metrics to a least-squares algorithm that has historically not been used due to classically limited computer resources. Modern computer resources (e.g., fast, arbitrary-precision arithmetic) have removed these limitations. This permits direct least-squares fitting for large rational polynomials. Fig. 1 shows a detail of a result described in Section IV that results from a direct least-squares fit using 1200 polynomial terms.

Next, I describe an extensive automatically generated library of every possible configuration of lumped circuit models up to and including five RLC elements. The library includes full synthesis equations to go from numerically evaluated rational polynomial coefficients directly to lumped element values without iteration for the 491 networks that have been solved to date with another 10 networks identified but as yet without synthesis equations. Synthesis equations are not possible for 122 of the networks in the catalog. The catalog is automatically searched to find the best circuit(s) that model the measured data. For simple cases, the specific components in and topology of the resulting lumped circuit can often be

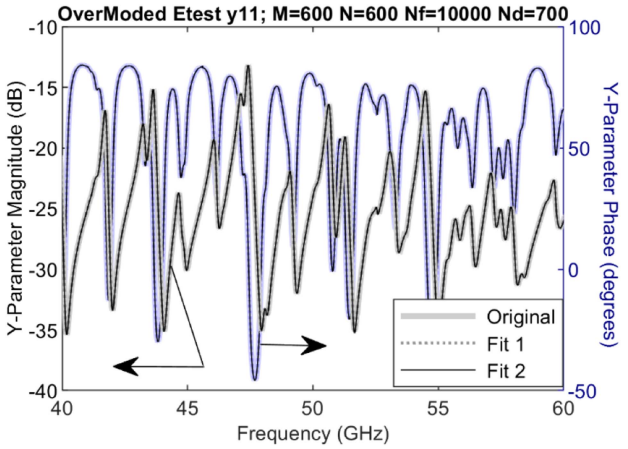

FIGURE 1. Detail from a 0.1–100 GHz direct rational polynomial least-squares fit using 600 terms in the numerator and in the denominator and a numerical precision of 700 digits in the mantissa. With Fit 1 and Fit 2 visually identical for both phase and magnitude, we verify that a sufficient number of rational polynomial terms and sufficient numerical precision has been used. Full frequency range is shown in Fig. 2.

correlated with the physical structure being modeled. Custom networks may be added as desired. Several approaches to extracting large circuit models from complex data are also suggested.

The transfer function rational polynomials, and the corresponding lumped circuits, are explored in terms of group theory, with application to extending the described circuit catalog and to extracting models from a fitted rational polynomial.

In this work, individual RLC elements are 'elements'. 'Networks' are networks of elements. Once specific RLC values are applied to a network, it becomes a 'component'. The generic configuration of the elements in a network is a 'topology'. The impedance and admittance characteristics as a function of frequency, represented using either symbolic or numerical coefficients, or as a list of numbers, are 'transfer functions'.

The entire MATLAB based direct rational model extraction and network library, CRCat (complex rational catalog), is freely available [5]. This is the result of work over 15 years.

II. LEAST-SQUARES ERROR METRICS

Our initial objective is to find a best fit rational polynomial model given the measured complex admittance samples, y_k, of a two-terminal device at frequencies ω_k. Such data is typically obtained from measured N-port scattering parameters. We wish to determine the coefficients of the best fitting rational polynomial in

$$\tilde{y}(s) = \frac{a_M s^M + \cdots + a_1 s + a_0}{b_N s^N + \cdots + b_1 s + b_0} \tag{1}$$

where $s = \sigma + j\omega$ and $a_m, b_n, \in \mathbb{R}$ for $0 \le m \le M$, $0 \le n \le N$.

For a physical circuit, the rational model coefficients must be real, as discussed in the next section, even though the data being fitted is complex. A typical least-squares fit of complex data provides complex polynomial coefficients. The unique least-squares fit reported here for the first time provides the best fitting real coefficients when fitting complex data. The standard least-squares approach determines the coefficients that minimize an error metric such as

$$|e^2| = \sum_k |y_k - \tilde{y}(j\omega_k)|^2 \tag{2}$$

For mean squared error, divide the above result by the number of samples. Substituting (1) into (2), we have

$$|e^2| = \sum_k \left| \frac{y_k \sum_n b_n (j\omega_k)^n - \sum_m a_m (j\omega_k)^m}{\sum_n b_n (j\omega_k)^n} \right|^2 \tag{3}$$

Minimizing the error is a non-linear problem due to the b_n coefficients in the denominator, and thus the usual least-squares algorithm cannot be invoked. Instead, non-linear optimization may be used, however, these algorithms are iterative, slow, and may become caught in local minima.

In addition, note that a small percentage error in $\tilde{y}$ contributes a large error when y_k is large, while small y_k samples contribute little to the total error regardless of their percent error. This has the advantage of suppressing the larger percentage noise typically present in small magnitude samples, however, since the admittance (or whatever transfer function is being fitted) might cover multiple orders of magnitude, it might be desirable to use an error metric that is proportional to the percent error in $\tilde{y}$ regardless of the magnitude of y_k.

We may linearize (2) by ignoring the denominator, [3], yielding

$$|e^2| = \sum_k \left| y_k \sum_n b_n (j\omega_k)^n - \sum_m a_m (j\omega_k)^m \right|^2 \tag{4}$$

This is now a standard, linear least-squares problem solved by inverting a matrix filled with appropriate statistics. This is closed form; no iteration is needed. However, this approach has been ignored in the past as the required statistics involve sums of samples multiplied by large powers of the frequencies. This quickly overwhelms typical numerical precision, especially when sample frequencies range over multiple orders of magnitude. In addition, instead of giving greater importance to large-value samples, this metric bestows importance on samples for which the numerator polynomial is large, regardless of the sample values.

In another approach, the denominator of (3) is replaced by an estimate of the denominator polynomial. For example, an estimate for the i^{th} iteration can be the result for the denominator polynomial of the previous iteration. The iterations can be started by using (4) to determine an initial estimate of the denominator polynomial, then proceeding to

$$|e^2| = \sum_k \left| \frac{y_k \sum_n b_n^{(i)} (j\omega_k)^n - \sum_m a_m^{(i)} (j\omega_k)^m}{\sum_n b_n^{(i-1)} (j\omega_k)^n} \right|^2 \tag{5}$$

This results in an iterative series of linear least-squares problems. The error metric typically used by Vector Fitting is closely related to (5) and the required polynomials are expanded in partial-fraction-like expressions bypassing typical numerical precision limitations. This has allowed wide application of Vector Fitting. As with (3), this metric bestows importance on large values of y_k.

A previously undescribed error metric is

$$|e^2| = \sum_k \left| \frac{y_k \sum_n b_n^{(i)} (j\omega_k)^n - \sum_m a_m^{(i)} (j\omega_k)^m}{\sum_m a_m^{(i-1)} (j\omega_k)^n} \right|^2 \tag{6}$$

As with (5), this also describes an iterative linear least-squares solution. Unlike (5), the denominator of this error metric normalizes each error term with an estimate of the numerator polynomial of $\tilde{y}$ from the previous iteration. In contrast to all previous error metrics, both terms of this error metric converge to unity. Thus, an equal percentage error in $\tilde{y}$ contributes an equal amount to the error metric regardless of the magnitude of the sample, y_k. This error metric could be used in an iterative linear least-squares algorithm. As with (5), this iteration could be started from the least-squares fit based on (4), but this time providing an initial estimate of the numerator. It could also be used in a modified form of Vector Fitting. It should be advantageous when the transfer function being fitted has a large dynamic range and small values of the transfer function are important.

In this paper, I explore the error metric (4), using modern computer capabilities. With appropriate modifications, any of these error metrics may be used in the approach described here.

III. DIRECT LEAST-SQUARES ALGORITHM

Given samples of a measured complex admittance, $y_k = g_k + jb_k$, at frequencies ω_k, we wish to find the real coefficients for a rational polynomial of the form

$$\tilde{y}(j\omega) = \frac{a_M (j\omega)^M + \cdots + a_1 (j\omega) + a_0}{b_N (j\omega)^N + \cdots + b_1 (j\omega) + b_0}, \quad a_m, b_n, \omega \in \mathbb{R} \tag{7}$$

that has minimum squared error according to (4).

The least-squares solution proceeds by filling, appropriately modifying, and then solving (8). Simplifying notation, all matrix elements in (11)–(13) are to be summed over all k measured data samples. The first term in (11) sums to the number of samples.

$$\begin{bmatrix} A_A & A_B \\ A_B^t & B_B \end{bmatrix} \begin{bmatrix} a \\ b \end{bmatrix} = [0] \tag{8}$$

$$a^t = [a_0 \quad a_1 \quad \cdots \quad a_M] \tag{9}$$

$$b^t = [b_0 \quad b_1 \quad \cdots \quad b_N] \tag{10}$$

$$A_A = \begin{bmatrix} 1 & 0 & -\omega^2 & 0 & \omega^4 & 0 & \\ 0 & \omega^2 & 0 & -\omega^4 & 0 & \omega^6 & \\ -\omega^2 & 0 & -\omega^4 & 0 & -\omega^6 & 0 & \cdots \\ 0 & -\omega^4 & 0 & \omega^6 & 0 & -\omega^8 & \\ \omega^4 & 0 & -\omega^6 & 0 & \omega^8 & 0 & \\ 0 & \omega^6 & 0 & -\omega^8 & 0 & \omega^{10} & \\ & & \vdots & & & & \ddots \end{bmatrix} \tag{11}$$

$$A_B = \begin{bmatrix} -g & b\omega & g\omega^2 & -b\omega^3 & -g\omega^4 & b\omega^5 & \\ -b\omega & -g\omega^2 & b\omega^3 & g\omega^4 & -b\omega^5 & -g\omega^6 & \\ g\omega^2 & -b\omega^3 & -g\omega^4 & b\omega^5 & g\omega^6 & -b\omega^7 & \cdots \\ b\omega^3 & g\omega^4 & -b\omega^5 & -g\omega^6 & b\omega^7 & g\omega^8 & \\ -g\omega^4 & b\omega^5 & g\omega^6 & -b\omega^7 & -g\omega^8 & b\omega^9 & \\ -b\omega^5 & -g\omega^6 & b\omega^7 & g\omega^8 & -b\omega^9 & -g\omega^{10} & \\ & & \vdots & & & & \ddots \end{bmatrix} \tag{12}$$

$$B_B = |y|^2 A_A \tag{13}$$

The superscript t indicates transpose.

All terms in (8)–(13) evaluate to real numbers, thus ensuring that the rational polynomial coefficients a_m, b_n are real. This form of least-squares appears to be previously unreported.

Dimensions of the matrices in (11) and (12) may be inferred from the size of their mating a_m and b_n vectors (9) and (10). The full matrix (8) is square of dimension $M + N + 2$, i.e., the number of unknown coefficients needed for the rational polynomial (7).

We are free to set one of the coefficients to a given value without loss of generality. This removes one dimension from the matrix and sets the right-hand side of (8). However, this results in a singular matrix when the value of the best fit for the selected coefficient is zero. Thus, after selecting a coefficient to set, we fill the matrix (8) and check the condition number. If the condition number indicates a singular matrix, we select a different term to hold constant. For large matrices, the condition number can be time-consuming to evaluate. In that case, an effective strategy is to limit the candidate coefficients to be evaluated.

On occasion, we wish to find the best fit for a rational polynomial corresponding to a specific RLC circuit that is missing one or more terms in the numerator or denominator. In this case, remove the rows and columns corresponding to the zero-valued coefficients. If one of the non-zero coefficients is known in advance (say, a DC value is known from measurement), appropriate modification can reduce the order of the least-squares matrix even further.

To improve the quality of the fit, we work with spectrally dense data sets, easily thousands of measured points. This is practical because each matrix element is a sum over all samples. In addition, there are many duplicate and near-duplicate elements in (4)–(6), further reducing required memory and effort. Evaluating a small set of 'sufficient statistics' is all that

is required to fill the matrix. These sufficient statistics need be evaluated only once when the same data is to be fitted to transfer functions of different orders.

The sufficient statistics are sums that include high powers of the radian frequency. With normal double precision, problems involving more than a small number of coefficients can result in catastrophic numerical precision errors. Variable precision arithmetic (vpa) provides a solution and is tested in the next section.

The rational polynomial (7) that is determined here has real coefficients. This guarantees that the model is causal (i.e., the real part is even and the imaginary part is odd) and that any complex poles are always present in exactly conjugate pairs. This does not force all poles and zeros to have a non-positive real part, required for stability, nor does it force the transfer function to have a non-negative real part at all frequencies. Adding one more condition, if all pure imaginary poles are simple and have a positive real residue, then a rational polynomial qualifies as a 'positive-real' function, or PR function [6]. These conditions are both sufficient and necessary for a rational polynomial to model a real passive lumped circuit [7] and can be checked, for example, by evaluating all poles and zeros, and if desired, modifying any positive real parts, and then reforming the modified rational polynomial.

IV. STRESS TESTING

One historical problem with using a standard least-squares algorithm is that it results in complex coefficients for the rational model. That problem is eliminated with the specialized least-squares algorithm of (8)–(13). A second problem is that the use of the usual numerical precision results in catastrophic numerical failure for all but the smallest problems. As seen in (11) and (12), the precision of the mantissa must be maintained for sums involving terms with frequency raised to zero power as well as frequencies raised to twice the power of the highest exponent in (7). Normalizing the frequency range to make full use of both negative and positive exponents is of limited benefit. In the past, extended precision arithmetic could be created for custom use, but it would be slow.

With the huge increase in computational speed that we have seen over the last 40 years, and with the availability of mathematical environments, e.g., MATLAB and others, fast variable precision arithmetic (vpa) is now available. I have implemented the least-squares algorithm of (8)–(13) in MATLAB using vpa. In this section, we explore the practical limits of this implementation for this problem.

MATLAB vpa allows the user to set the number of digits in the mantissa of the vpa data type. The exponent for the vpa format is essentially unlimited. A simple circuit that provides an extreme test case is shown in the lower right corner of Fig. 2. It is an open circuited stub 0.5 × 2 mm on an $\varepsilon_r = 10$ substrate with an area of 5 × 10 mm, thickness 1 mm, loss tangent 0.005, and air above 5 mm thick. The stub metal is copper, conductivity 5×10^7 S/m. EM analysis cell size is 0.05 mm. For an extreme test, I analyzed the response from 0.01 – 100 GHz, every 0.01 GHz for 10,000 data points. Above

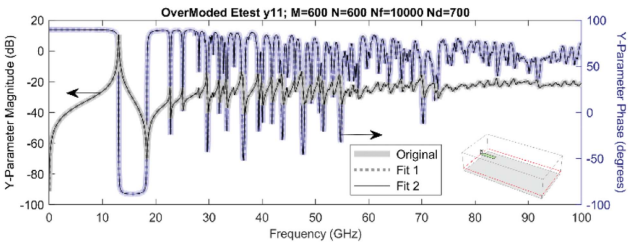

FIGURE 2. The full 0.1–100 GHz rational polynomial fit. With Fit 1 and Fit 2 visually identical for both phase and magnitude, we verify that a sufficient number of rational polynomial terms (M, N) and sufficient numerical precision (Nd) has been used to fit the 10,000 frequency points in the data set. A detail of this fit is shown in Fig. 1.

20 GHz, the conducting box containing the circuit becomes a highly over-moded resonator, presenting an exceptional modeling challenge. Data to be fitted was generated by the Sonnet [8], [9] EM analysis.

There are two expected failure modes: 1) Insufficient number of coefficients in the rational polynomial, and 2) Insufficient numerical precision. To test each failure mode, I performed two fits: 1) Fit 1 takes the Sonnet EM data and performs a fit splitting a specified number of coefficients evenly between numerator and denominator, and 2) The rational polynomial resulting from Fit 1 is then evaluated over the same frequencies and that fitted transfer function is then itself fitted, yielding Fit 2. If there is insufficient precision, then Fit 2 will not match Fit 1. If there are an insufficient number of coefficients or insufficient precision, then Fit 1 will not match the data being fitted.

Fig. 2 shows Y-parameter magnitude and phase for the original EM data compared to both fitting results for 1200 coefficients (600 in the numerator and 600 in the denominator) and 700 digits of mantissa precision. It works. Fit 1 RSS error (based on (2)) is 4×10^{-5}. Results with this level of error always give visually identical results when plotted. The Fit 2 versus Fit 1 RSS error is 6×10^{-11} indicating no additional numerical precision is needed. Fig. 1 shows expanded detail from Fig. 2 over a small frequency range. A MATLAB 'fig' file accompanies this paper [5] allowing the reader to interactively explore this large data set in fine detail.

Nearly identical plots were obtained using as few as 700 coefficients, except for several narrow spurious resonances in the fitted transfer function, some of which were prominent. It is as if the fit realized minimum error by pushing all the error to just a few points with the remaining fit precisely matching the input data.

One must be sure to provide input data dense enough that these narrow 'error' resonances do not hide in between data points. To check for this failure mode, I also evaluated and plotted all transfer responses at 50,000 frequencies. These results precisely overlaid the 0.01 GHz frequency step initial data.

CPU time for a 1200 coefficient fit using 700 digits in the mantissa is two to three hours. Numerically, frequency was

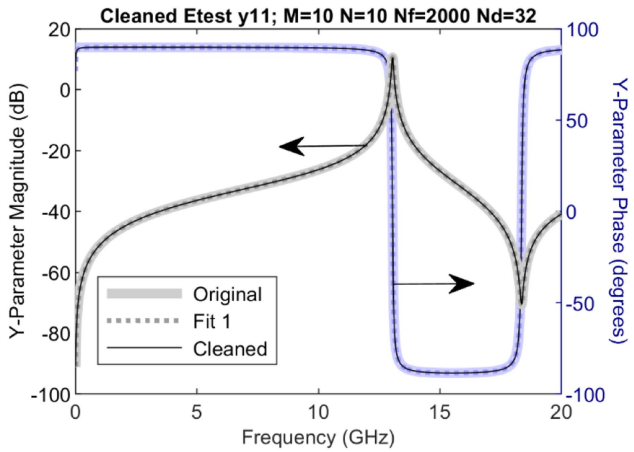

FIGURE 3. The data of Fig. 2 was restricted to the first 2000 frequency points covering 0–20 GHz, with a good fit realized using 10 terms in the numerator and denominator, and 32 digits of precision in the mantissa, requiring six seconds of analysis time. The result was 'cleaned', i.e., any positive real parts in any poles or zeros were set to zero. There is no visual change in the modeled result.

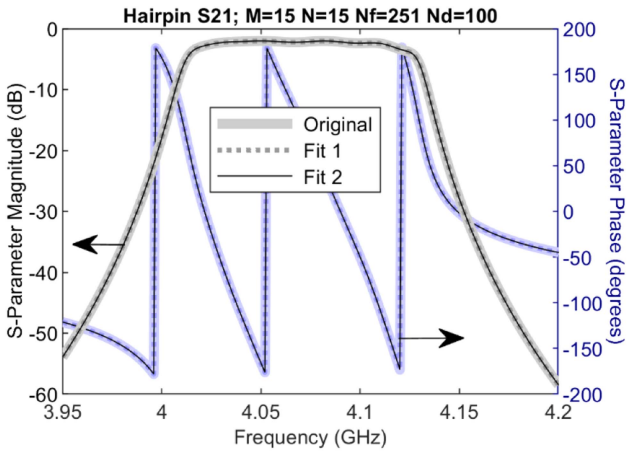

FIGURE 4. Result of fitting a rational polynomial to EM analysis data only over this filter's pass band from 3.95 to 4.2 GHz with 251 data points calculated. We achieve a Fit 1 with error of 2×10^{-9} indicating we are using a sufficient number of rational polynomial terms (30) and a Fit 2 error of 2×10^{-18} indicating that 100 digits of mantissa precision is sufficient.

raised to the power of 1200 with 700 digits of mantissa precision providing sufficient accuracy. For large problems, CPU times vary by as much as a factor of two for identical runs with no other loading on the subject mid-range notebook computer executing one core. When timing results vary, approximate analysis times are reported.

I also performed fits over a subset of this data, 0.01 – 20 GHz. A good fit requires 20 coefficients and 32 digits of precision and results in a fitting error of 1.4×10^{-4}, Fit 1 in Fig. 3. Fitting time was six seconds.

Evaluation of the required statistics in (11) and (12) varies linearly with number of transfer function samples. Least-squares matrix solve time varies with the cube of the number of coefficients. The overall fitting time varies linearly with the number of digits used in the arithmetic.

Extraction of poles and zeros from the rational polynomial can also be used to evaluate amplifier stability [10].

When I evaluate the poles and zeros of the fitted polynomials for the 20 GHz results, I found only one zero and one pole with positive real parts, and they were small. Setting them to zero resulted in no visible change in the response. Fig. 3 shows the 20 GHz model 'cleaned' in this manner. This cleaning of the poles and zeros was also attempted for up to 300 coefficients on full 100 GHz models without yielding a useful result presumably because there was an insufficient number of terms in the fitted rational polynomial. Extracting poles and zeros for more coefficients would require a few hours of CPU time and was not attempted.

As illustrated above, this least-squares fit can require arithmetic using hundreds of digits to avoid potentially catastrophic failure due to insufficient numerical precision for the matrix inversion as the numerical values in the matrix can range over hundreds of orders of magnitude. This situation is typical when fitting rational polynomials with, for example, hundreds of terms. In this case, the final result is the rational polynomial itself. Converting large rational polynomials into a generic RLC circuit can be realized by performing a partial-fractions expansion followed by the approach discussed in [1] and [2] and is not the topic of this paper.

V. BAND LIMITED DATA TEST

The 'Hairpin Filter' layout from the Sonnet Suites example folder [8] illustrates fitting a rational polynomial to narrow passband data. In this case, we EM analyze the filter only over its pass band from 3.95 to 4.2 GHz with 251 data points calculated. Fig. 4 shows a Fit 1 with error of 2×10^{-9} and a Fit 2 error of 2×10^{-18} using 100 digits of mantissa precision. With 32 digits, the Fit 1 error is about the same, but the Fit 2 error increases to 4×10^{-9}. Analysis time for both cases is 3 seconds.

Rational polynomials can perform limited extrapolation. To explore this, I took the rational polynomial from the above fitting, which is based only on the narrow bandpass data, and I extrapolated it, Fig. 5. At least for this circuit, extrapolation works well when the data is above the EM analysis noise floor of –200 dB from 2.5 GHz to 6 GHz. The extrapolation misses the second order response at 8 GHz, as expected.

Cleaning the poles and zeros, i.e., removing any positive real parts, failed to provide useful results for this circuit. The EM data for this filter was de-embedded, removing the port-connecting transmission lines. Reference planes were set on each port at the start of the physical filter. It is possible that the de-embedding, and/or the distributed nature of the filter caused the failure of the pole/zero cleaning. It is also possible that simply using more terms in the rational polynomial would have solved the problem. These hypotheses have not been investigated.

If rational polynomial results are to be used for time domain analysis, solving for the roots, setting the real parts to zero,

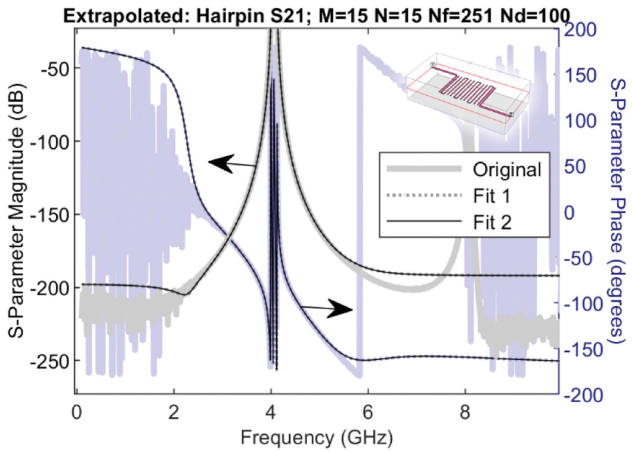

FIGURE 5. Fitting to the same, limited pass-band data used in Fig. 4, extrapolation of the fitted rational polynomial filter response matches EM analysis data well into the filter stop-band, failing only when the EM data is well below the –200 dB EM numerical noise floor, or when the frequency is approaching the second order filter response.

and re-forming the rational polynomial should assure a stable result. To assure an accurate result, one should check that the new transfer function exhibits a satisfactory match to the original data. This process is easily implemented with standard MATLAB functions. From the above results I infer that this cleaning process can be practical for transfer functions that require fewer than a few hundred coefficients and are fitted to data starting at low frequency.

For this test, I fitted rational polynomials to the S-parameters. Note that rational polynomials representing S-parameters of a physical device are typically not positive-real, but must still be causal (i.e., the coefficients must be real) and stable (all poles and zeros must have non-positive real parts). The S-parameter condition for passivity ($|S| \leq 1$) is equivalent to the positive-real function condition of the real part of the impedance or admittance being non-negative.

VI. OBSERVATIONS ON GROUP THEORY

The set of complex rational polynomials (1) form a field (in the group theory sense) under addition, subtraction, multiplication, and division, with closure, associativity, distributivity, and an inverse that yields an identity element for each operation and for every member [11]. In this paper, we work with a countably infinite (there are 623 non-trivial members with five or fewer lumped elements) set of rational polynomials that represent the admittance or impedance of two-terminal lumped circuits. These rational polynomials take the form of (1) with $s = j\omega$ and real coefficients, i.e., $a_m, b_n \in \mathbb{R}$, that are a function of R, L, and C only. Real coefficients force a causal transfer function. Two rational polynomial transfer functions are the same set member if they are algebraically equal.

I introduce nomenclature for these sets as Y_1 and Z_1 where rational polynomials in Z_1 are the algebraic inverse of those in Y_1 with the homomorphism $Z_1 \leftrightarrow Y_1$ that satisfies $z \leftrightarrow 1/y \ \forall \ z \in Z_1, \ y \in Y_1$. Due to this homomorphism, we can switch seamlessly between sets depending on whether we are dealing with admittance or impedance.

Anticipating possible extension of this group theory to cover lumped circuit transfer functions with more than two terminals, I use the subscript '1' above to signify that we are working with a 1×1 matrix, which amounts to a 1-port device (one terminal can be viewed as 'ground'). If there are three terminals, then we need a 2×2 matrix to specify all required admittances, with one of the three terminals arbitrarily being treated as 'ground', resulting in a 2-port device. Handling RLC networks that have more than three terminals in terms of impedances requires special consideration because we live in a universe in which electric current predominates [12].

To illustrate, two members (referred to in Sections IX and XI) of the set Y_1 are: (14) and (15), shown at the bottom of the next page.

The coefficients of each member in these sets are formed only from symbolic RLC values and each polynomial is a function only of $j\omega$. The topologies of these two networks, XIII and XIV, are illustrated in the top row of Fig. 6.

To form groups, two binary operators, which we designate by $\oplus$ and $\otimes$, are useful. The first operator indicates adding two members of a set. For Z_1, this corresponds to connecting impedances in series and for Y_1, connecting admittances in parallel.

Normal algebraic multiplication of set members is not useful for this work. Instead, the second operator indicates the algebraic inverse of the sum of the algebraic inverses of each of two members. Within Z_1, this corresponds to connecting impedances in parallel and within Y_1, connecting admittances in series.

To form a group, we need identity elements. The identity element for $\oplus$ in both sets is a rational polynomial with zero in the numerator and any non-zero polynomial in the denominator, the 'zero rational polynomial'. The identity element for $\otimes$ in both sets has zero in the denominator and any non-zero polynomial in the numerator, the 'infinity rational polynomial'. For closure, we must include the difference between two identical infinity rational polynomials, the 'indeterminate rational polynomial', zero over zero. In addition, for closure, we must include all transfer functions for all trivial networks, e.g., two resistors in series, etc., even though they are not included in the CRCat catalog.

Both $\oplus$ and $\otimes$ have the same inverse, the negative of the original rational polynomial. The inverse may also be obtained by changing the sign of every RLC element in the rational polynomial. Applying either $\oplus$ or $\otimes$ to any member of Y_1 or Z_1 and its inverse yields either the corresponding identity member or, in one case, the indeterminate member.

Supplemented as described above, both Y_1 and Z_1 have an identity element, an inverse, commutativity, associativity, and closure for both operators and for all members and thus each forms a group.

As described above, negative RLC elements are required if we are to have an inverse. While negative elements are not

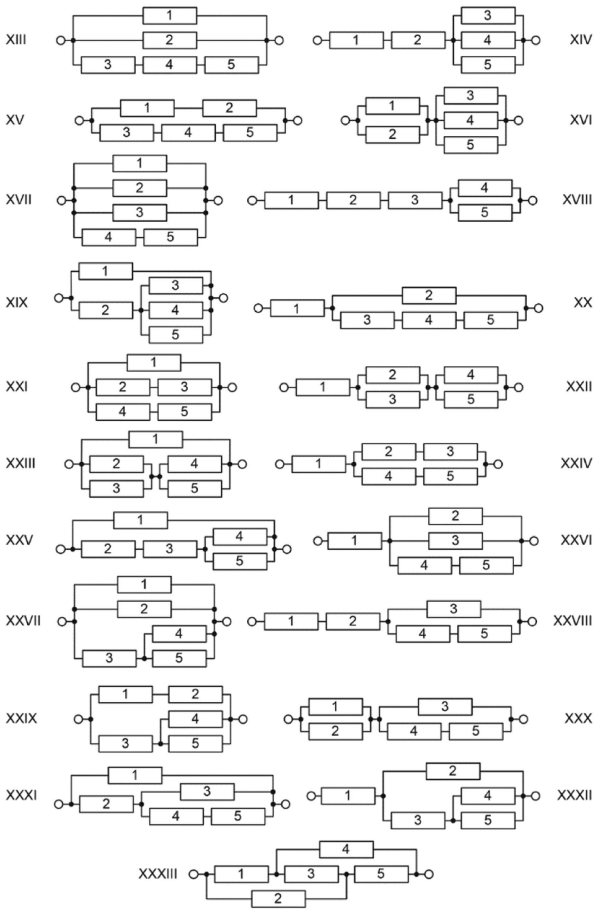

FIGURE 6. All possible five-element topologies. Uniquely among these topologies, XXXIII cannot be formed by successive series and parallel connections.

physical, they are required in numerous applied de-embedding situations. Note that a passive, positive-real rational polynomial can result even with negative valued lumped elements in some situations, e.g., Fig. 5 in [4].

These sets and the operators $\oplus$ and $\otimes$, form groups, but they do not form a field (in the group theory sense) as the operations are not distributive. For example, illustrating the distributive property using three members of Z_1: an R, an L, and a C:

$$z_R \otimes (z_L \oplus z_C) \neq (z_R \otimes z_L) \oplus (z_R \otimes z_C). \tag{16}$$

In words, a resistor connected in parallel with a series LC is not the same as a parallel RL connected in series with a parallel RC. Therefore, the distributive property does not hold for the sets Z_1 and Y_1.

In addition to these transfer functions, this group theory also applies to the set of all two-terminal networks, for which I propose the terminology N_{W1}, and the set of topologies, T_{P1}, provided we supplement both sets with 'anti-networks' and 'anti-topologies' that exactly cancel an identical non-anti-network or topology when connected either in series or in parallel. For both groups, the $\oplus$ operator refers to connecting elements in series and the $\otimes$ operator to connecting elements in parallel. An example of a member of N_{W1} is n_{XIII-1}, and of T_{P1} is t_{XIII}.

VII. BUILDING NETWORK LIBRARIES

All possible three- and four-element topologies are diagramed in Fig. 2 of [4], and all possible five-element topologies are diagramed here in Fig. 6. Most topologies are formed from a combination of topologies of fewer elements by the $\oplus$ and $\otimes$ operators.

I propose determining all possible topologies of a given number of elements, N, by assembling them from smaller topologies in T_{P1} using the $\oplus$ and $\otimes$ operators. For example, one way to form topology XXXI (Fig. 6) is by connecting a one-element topology in parallel with XII (Fig. 2 in [4]). A methodology is advantageous because the number of possible topologies increases rapidly for topologies of five or more elements:

1) Given knowledge of all possible smaller topologies ($N-1$ and fewer elements), assemble all possible topologies that total N elements by using all possible combinations of those networks with the $\oplus$ and $\otimes$ operators that result in N elements.
2) Search for unique topologies that cannot be formed using $\oplus$ and $\otimes$.
3) Eliminate all trivially equivalent topologies.
4) Populate the assembled topologies with all possible combinations of RLC elements.
5) Eliminate all trivially reducible networks within each topology.

Illustrating step 1 for $N = 5$, consider all combinations of $N = 4$ with $N = 1$ topologies and of $N = 3$ with $N = 2$ topologies. There is no need to consider $N = 3$ combined with two $N = 1$ topologies as all $N = 3$ and $N = 1$ topology combinations were already considered in determination of the $N = 4$ topologies. Topologies to be eliminated include, for example, those with more than three elements all in series, or all in parallel.

$$y_{XIII-1} = \frac{CL_aL_b(j\omega)^3 + C\left(L_aR_a + L_aR_b + L_bR_a\right)(j\omega)^2 + \left(L_a + CR_aR_b\right)j\omega + R_a}{CL_aL_bR_a(j\omega)^3 + CL_aR_aR_b(j\omega)^2 + L_aR_aj\omega} \tag{14}$$

$$y_{XIV-2} = \frac{LC_bR_b(j\omega)^3 + L(j\omega)^2 + R_bj\omega}{LC_bR_aR_b(j\omega)^3 + L\left(R_a + R_b + \frac{C_bR_b}{C_a}\right)(j\omega)^2 + \left(\frac{L}{C_a} + R_aR_b\right)j\omega + \frac{R_b}{C_a}} \tag{15}$$

TABLE 1. Populating Topologies With Elements

XIII-XVIII	XXI-XXIV	XXV-XXVI	XVII-XXX
1-RLRLC	1-RRLRL	1-RRLRL	1-RLRRL
2-RCRLC	2-RRLRC	2-RRLRC	2-RLRRC
3-LCRLC	3-RRLLC	3-RRLLC	3-RLRLC
	4-RRCRC	4-RRCRL	4-RLLRL
XIX-XX	5-RRCLC	5-RRCRC	5-RLLRC
1-RRRLC	6-RLCLC	6-RRCLC	6-RLLLC
2-RLRLC	7-LRLRL	7-RLCRL	7-RLCRL
3-RCRLC	8-LRLRC	8-RLCRC	8-RLCRC
4-LRRLC	9-LRLLC	9-RLCLC	9-RLCLC
5-LLRLC	10-LRCRC	10-LRLRL	10-RCRRL
6-LCRLC	11-LRCLC	11-LRLRC	11-RCRRC
7-CRRLC	12-LLCLC	12-LRLLC	12-RCRLC
8-CLRLC	13-CRLRL	13-LRCRL	13-RCLRL
9-CCRLC	14-CRLRC	14-LRCRC	14-RCLRC
	15-CRLLC	15-LRCLC	15-RCLLC
	16-CRCRC	16-LLCRL	16-RCCRL
	17-CRCLC	17-LLCRC	17-RCCRC
	18-CLCLC	18-LLCLC	18-RCCLC
		19-CRLRL	19-LCRRL
		20-CRLRC	20-LCRRC
		21-CRLLC	21-LCRLC
		22-CRCRL	22-LCLRL
		23-CRCRC	23-LCLRC
		24-CRCLC	24-LCLLC
		25-CLCRL	25-LCCRL
		26-CLCRC	26-LCCRC
		27-CLCLC	27-LCCLC

All topologies in Fig. 6 were found as described above except topology XXXIII, a Wheatstone bridge-like topology, which cannot be formed using only $\oplus$ and $\otimes$. A methodology for finding these unique topologies remains an open question that should be resolved prior to proceeding to an exhaustive $N = 6$ enumeration, where such topologies promise to be numerous.

To illustrate step 4, topology XIII, Fig. 6, can be non-trivially populated by three combinations of RLC elements, with each element listed in order: 1) RLRLC, 2) RCRLC, and 3) LCRLC. These populations are listed at the top of the first column of Table 1. Note, there is only one way to non-trivially populate the three elements connected in series and that restricts the number of non-trivial populations to the three ways to populate two elements in parallel. These networks are referred to respectively as XIII-1, XIII-2, and XIII-3.

Continuing, there are three ways to populate each of XIII – XVIII, nine ways to populate each of XIX and XX, 18 ways to populate each of XXI – XXIV, 27 ways to populate each of XXV – XXX, and 81 ways to populate each of XXXI – XXXIII. Table 1 lists all the ways to populate all the topologies except XXXI – XXXIII. A spreadsheet listing all these network populations is included with the software download associated with this article.

Populating a topology with RLC elements yields a member of the set N_{W1}. The corresponding impedance transfer function is a member of the set Z_1, and the admittance transfer function is a member of the set Y_1. The mapping between all members of N_{W1}, Z_1, and Y_1 are one-to-one. The mapping of members of each of these three sets to T_{P1} is many-to-one.

TABLE 2. Complete List of Transfer Function Signatures

1-1	1010-11111	111-101	1111-1111
1-10	10101-1010	111-11	1111-11110
1-11	10101-101010	111-110	1111-11111
10-1	10101-11111	111-111	11110-1111
10-101	101010-10101	111-1110	11110-11111
10-11	11-1	111-1111	11111-1010
10-111	11-10	1110-111	11111-10101
101-10	11-11	1110-1111	11111-1110
101-1010	11-110	1110-11111	11111-1111
101-111	11-111	1111-101	11111-11110
101-1111	110-11	1111-1010	11111-11111
1010-101	110-111	1111-110	
1010-10101	110-1111	1111-111	
1010-1111	111-10	1111-1110	

VIII. THE NETWORK LIBRARY

Given all possible 1 – 5 element topologies, populating them with all possible combinations of RLC elements and eliminating all trivially redundant networks, we have 623 networks. Adding a network to the catalog starts by specifying a netlist. Instead of evaluating the network admittance numerically, CRCat evaluates the admittance symbolically, using the MATLAB symbolic math functionality. The admittance is reduced to a symbolic rational polynomial and stored in a data structure for that network. If possible, synthesis equations are then derived, again using MATLAB's symbolic math functionality. These equations are used to convert numerical values from the best fit rational polynomial coefficients into numerical values for the RLC elements as detailed in the next section.

The usual approach to obtaining the best fitting RLC values of a network is to invoke a non-linear optimization. Such an approach would be far too time-consuming and prone to failure to be used on all 623 networks. These synthesis equations enable a fast, accurate solution.

The form of the transfer function polynomial for each network is stored in the network's data structure as a field 'flagSig', and is called the 'signature'. For example, the signature for a rational polynomial that is quadratic in both numerator and denominator, but lacking a constant (DC) term in the denominator is '111-110'.

Table 2 lists all 53 unique signatures present among all 623 networks in the base catalog. Each of these signatures are consistent with requirements for a rational polynomial for a lumped circuit [7]. The list includes all signatures that are possible for networks of one to five elements.

In addition to a name, like XIII-3, each network can be referred to by an identifying number. For example, XIII-3 is the 122nd network in the CRCat catalog and is thus also known as 'CR122', which is compactly written as 'XIII-3/122'.

IX. COMPONENT EXTRACTION

The rational polynomials in Y_1 and Z_1 sets cannot represent all possible rational polynomials. Rather, given a rational polynomial that has been fitted to our desired data, our task is to find the rational polynomial(s) in these sets that best represent(s) the fitted data.

To determine the RLC values for a such a network, CRCat performs a least-squares fit on a given noisy measured data set for the form of the rational polynomial that corresponds to that network as specified by the polynomial signature for that network.

For example, XIII-1, CR120, the network whose transfer function is given above in (14), has a signature of '1111-1110'. To determine the RLC values in a given (noisy) data set that best correspond to that transfer function, MATLAB is tasked as described in Section III to perform a least-squares fit that yields numerical values for the coefficients of the form

$$y(\omega) = \frac{a_3(j\omega)^3 + a_2(j\omega)^2 + a_1(j\omega) + a_0}{b_3(j\omega)^3 + b_2(j\omega)^2 + b_1(j\omega) + 0}. \tag{17}$$

The fit (8) is set to force the value of b_0 to be zero for XIII-1, which has a zero constant term in its denominator. It is also normalized so that $a_0 = 1$. Once we have numeric values from the least-squares fit, we can now set those values equal to the normalized symbolic coefficients of (14), forming a set of non-linear simultaneous equations,

$$a_3 = CL_aL_b/R_a \tag{18}$$

$$a_2 = C\left(L_aR_a + L_aR_b + L_bR_a\right)/R_a \tag{19}$$

$$a_1 = \left(L_a + CR_aR_b\right)/R_a \tag{20}$$

$$b_3 = CL_aL_b. \tag{21}$$

$$b_2 = CL_aR_b. \tag{22}$$

In populating the data structure for XIII-1, this set of five non-linear equations in five variables has been solved symbolically by MATLAB to yield the synthesis equations for the RLC values. The least-squares determined coefficients then directly and quickly determine the RLC values. This is much faster than attempting a problem prone iterative optimization of the RLC values of XIII-1 to match the measured data.

There are six unknown coefficients in the transfer function (14) after normalization and only five unknown RLC values. In some cases, the derived synthesis equations do not match one or more of the coefficients that were not used in deriving the synthesis equations. Thus, every synthesis solution must be checked to see if it yields the original polynomial equation. If it does not, then a different set of coefficients must be used. For example, remove (18) and add an equation for b_1.

The RLC element values that result from fitting a given transfer function can be negative, but the transfer function is still always perfectly causal. Negative valued elements might or might not yield positive-real results. This can be tested by a CRCat function that, using symbolic math entirely, takes the real part of the transfer function and checks for zero crossings.

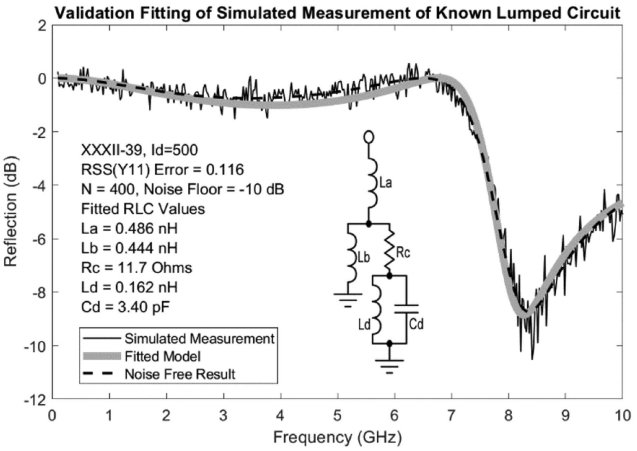

FIGURE 7. For validation, we start with the indicated circuit, add noise to simulate measurement with a –10 dB noise floor, and then select the best fitting model. The values of the original circuit are 0.5 nH, 0.4 nH, 10 Ohms, 0.2 nH, 3 pF. Among all 623 circuits in the base library, the original network provides the best fit. With a –20 dB noise floor, the fitted result is visually identical to the original data.

If desired, any equivalent networks (described in the next section), might provide all positive element values.

Complex element values are rare but might happen when the network's synthesis equations exhibit multiple solutions, i.e., when more than one set of element values yield identical transfer functions. In this case, if there is a complex element value in one solution, its complex conjugate is observed in the other. As with all fitting solutions obtained as described in this paper, the network response is always perfectly causal. Since complex element values might be difficult to use, transformation to a different, equivalent network often remedies this cosmetic problem.

Synthesis equations for a subset of the networks considered here were previously derived and published in [7], all members of the Ladenheim Catalogue [13]. The download [5] accompanying this paper includes a spreadsheet mapping the Ladenheim Catalogue to this catalog including a list of all related equivalent and degenerate networks, and, in a separate document, the schematic of each network involved.

The transfer function is evaluated using the best fitting values of the RLC elements and the fitting error is calculated (2). Given a measured transfer function, this process is repeated for all possible networks in the base catalog, as well as any user specified networks in the custom catalog. The best fits of those networks are then displayed in schematic form along with RLC values. The user may then select the component that is most appropriate for their requirements.

To test this capability, I selected network XXXII-39, CR500, and numerically evaluated the transfer function. To this I added noise yielding a –10 dB noise floor, the level needed to realize a noticeable extraction error. I applied that data to the extraction algorithm described above and of all 623 networks, XXXII-39 provided the best fit, Fig. 7. Dropping

the noise floor to –20 dB makes the original and extracted data visually identical.

For measured (i.e., noisy) data of an unknown circuit, the extraction algorithm fits the form of the rational polynomial for every possible network in the library and then uses the corresponding pre-solved and stored synthesis equations to evaluate the required RLC values for each network. These values are then substituted into the symbolic equation for the network transfer function and mean squared error is calculated. The best fit components of all the networks in the catalog are then displayed. If an adequate (as subjectively determined by the user) component exists in CRCat, this algorithm will find it.

X. NETWORK RELATIONSHIPS

In the course of developing the CRCat catalog, I discovered multiple relationships between networks. These include:

1) Equivalent relationships: Each network in a pair can be transformed into the other.
2) Degenerative relationships: A network can be transformed into another network with fewer elements. The smaller network cannot be uniquely transformed back into the larger network.
3) Regenerative relationships: A network can be uniquely transformed into a network with more elements. However, the larger network cannot in general be transformed into the smaller network.
4) Compound relationships: A degenerate network transforms into a network with fewer elements that is a regenerative network, which then transforms into a different larger network.

Each member of an equivalent network pair can be transformed to the other, each with the same transfer function. Each member of an equivalent pair must be a 'canonical', or 'minimal network', i.e., it cannot be exactly represented with fewer elements. There are now 3602 known transforms between equivalent network pairs in CRCat of which 275 remain unsolved. There are another 234 suspected transforms that, if they exist, would be half of an equivalent pair. Zverev [14] reports 28 equivalence transforms for 14 network pairs and details their critical use in filter design.

A trivial example of a degenerate network is two resistors in series, which degenerates into one resistor. One resistor cannot be uniquely transformed back into two resistors. Trivially degenerate networks are not included in CRCat. There are 465 non-trivial degenerate network transforms among 132 degenerate networks in CRCat. There are no degenerate networks with three or fewer elements. Zverev [14] reports one degenerate transform. If a network degenerates into one member of a set of equivalent networks, then it typically degenerates into all members of that set. Degenerate networks are always 'non-canonical' or 'non-minimal', in that their transfer function can be exactly represented by a minimal network with fewer elements.

A trivial example of a regenerative network is a single capacitor can regenerate into a special case of a series RC circuit provided the R of the series RC has zero value. Note that a general series RC (i.e., those with an R of any value) cannot be transformed into an equivalent C. Trivial regenerative network transforms are not stored and are identified only when both networks have the same polynomial signature. There are 421 non-trivial regenerative network transforms, of which 20 still have unknown transform equations. It appears that regenerative transforms have not been previously reported.

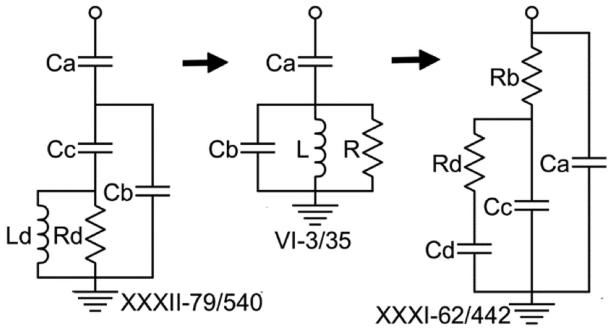

FIGURE 8. A typical compound relationship between networks. The first network is non-minimal and thus cannot be equivalent to any other network. However, it does degenerate to the middle network, which can then regenerate special cases of the third network. If we did not know about the middle network, it would seem to be a one-way 'equivalence' from the first to the third network.

There are transforms for 163 compound relationships of which 11 still have unknown transform equations. If the smaller network regenerates into a set of equivalent networks, then the compound relationship typically exists with all members of the equivalent set. It appears that compound relationships between networks have never been previously reported.

A compound relationship example is XXXII-79/540(5)→VI-3/35(4)→XXXI-62/442(5), Fig. 8, where a five-element non-minimal network degenerates into a minimal four-element network, which then regenerates into a minimal five-element network. If the initial CR540→CR35 transform was not known, then CR540→CR442 (which is solved and stored in the data structure for CR540) would appear to be a one-way 'equivalence' relationship, which seems impossible. There are other networks equivalent to each of CR35 and CR442 that participate in related, intertwining relationships.

The existence of a transform from one network to another is tested by setting specific RLC values for the first network, evaluating the component's response, and then fitting the second network to that response. This is a 'fitting test'. When the transfer function of the fitted component (i.e., a network with specific element values specified) matches the transfer function of the original component to within numerical precision, MATLAB *solve* is used to derive the symbolic expressions to yield the transform equations.

Synthesis equations (i.e., the equations that determine the element values given the fitted rational polynomial coefficients) must be available for the network being fitted. Thus,

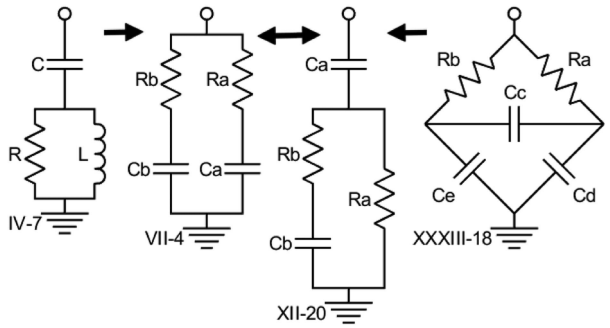

FIGURE 9. Four of the 17 three- to five-element networks with a polynomial transfer function signature of '111-110'. The first one, IV-7, CR27, has no equivalent networks, but its transforms can regenerate a non-trivial special case of the second, VII-4, CR39, but not the third, XII-20, CR112 (see text). The middle two are equivalent, and the last one, XXXIII-18, CR560, degenerates into either of the middle two.

the fitting test requires the second network to have a synthesis solution. There is no synthesis solution for non-minimal networks because there is no unique solution. Given this situation, a unique transform into that network impossible. If *solve* does not find a synthesis solution, it is usually for this reason.

However, it is possible that *solve* is unable to find a synthesis solution for a minimal network. In this case, transforms into such networks will not be detected. By observing patterns in the relationships of associated networks, we infer that there might exist synthesis equations for 10 five-element networks that would result 234 additional transforms. There are a total of 491 networks with synthesis equations and 132 without.

If a component is populated with element values and the network has multiple synthesis solutions, you can obtain an alternative, equivalent set of element values by executing the above-described fitting test.

All identified equivalences for up to four elements are listed in Table 1 of [4]. This list is likely complete. All known transforms involving five-element networks are stored in CRCat in the data structure for each network. For example, Fig. 9 illustrates four networks of a total of 17 that have the polynomial signature '110-111'. The first one, IV-7, CR27, has three elements and has no other equivalent networks. The next two, VII-4, CR39, and XII-20, CR112, both have four elements and are equivalent to each other, along with four other four-element networks (not shown). Then there are 10 five-element 'degenerate' networks with one of them, XXXIII-18, CR560, illustrated. These can all be simplified to any of the six equivalent four-element networks. Degenerate networks are included in this work so that when encountered, they may be quickly recognized and simplified as desired.

The first network, IV-7, CR27, can regenerate into a special case of the second network, VII-4, CR39. The second network cannot in general be transformed into the first because a four-element network can represent a wider range of transfer functions than a three-element network even though the three-element network can represent a portion of the four-element network transfer functions.

The third network, XII-20, CR112, is equivalent to the second and technically can also be regenerated from the first. However, when doing so with the specific element values used to fit test the first network, the resulting element values exceed the numerical precision of the component, and the fitting test failed. Thus, it is not included in the group of networks that the first network can regenerate.

We can indicate two-way transfer function equivalences and one-way degeneracies and regeneracies symbolically using group notation, for example:

$$n^{(3)}_{IV-7} \rightarrow n^{(4)}_{VII-4} \leftrightarrow n^{(4)}_{XII-20} \leftarrow n^{(5)}_{XXXIII-18} \tag{23}$$

where lower case 'n' indicates a member of the N_{W1} network group. Here, the number of elements is shown in the superscript, which helps in identifying the type of transform indicated.

Symbolic equations for 4345 identified degenerate, regenerate, equivalent, and compound network transforms are included in the data structure for each network with another 306 transforms known to exist but not yet solved. Symbolic equations for the poles and zeros of each network are also generated and stored in CRCat.

To populate the CRCat data structure for a network with these equations, the user specifies RLC element variable names and provides a net list for their connection. From that point on, everything is automatically evaluated and stored in the data structure for that network. Performing this evaluation for all 623 networks of the base CRCat catalog requires about one week of near continuous computer time on a mid-range notebook computer using one core. Adding several custom networks to CRCat typically requires just a few minutes.

XI. DUALITY

Network topologies on the same row in Fig. 2 of [4] and Fig. 6 here are dual topologies. The transfer function of one topology is obtained by a change of variables in the transfer function of the other. Specifically, in the dual topology, change all capacitors to inductors, all inductors to capacitors, invert all resistances, and conclude by inverting the entire transfer function. In fact, the circuits XIII-1 (populated with RLRLC) and XIV-2 (populated with RCRLC), whose transfer functions are above in (14) and (15) and whose topologies are in the top row of Fig. 6, are duals.

Intriguingly, when a topology can be described in terms of individual elements connected using only $\oplus$ and $\otimes$, the dual topology is formed by swapping operators. Continuing with the same two example networks, we see in Fig. 6 that topology XIII is two elements connected in parallel with a series connection of three elements. The dual topology of XIII is XIV, two elements connected in series with three elements connected in parallel. Using the topology group operators:

$$t_{XIII} = t_1 \otimes t_1 \otimes (t_1 \oplus t_1 \oplus t_1) \tag{24}$$

$$dual(t_{XIII}) = t_1 \oplus t_1 \oplus (t_1 \otimes t_1 \otimes t_1) = t_{XIV} \tag{25}$$

where lower case 't' indicates a member of the set T_{P1}, and t_1 indicates the sole one-element member of that set.

A subscript '2p' indicates the set member with two elements in parallel (i.e., $t_{2p} = t_1 \otimes t_1$) and '2s', two elements in series (i.e., $t_{2s} = t_1 \oplus t_1$). Using the transfer function group operators, the transfer functions (14) and (15) are concisely written as:

$$y_{XIII} = y_{Ra} \otimes y_{La} \otimes (y_{Rb} \oplus y_{Lb} \oplus y_C) \tag{26}$$

$$z_{XIV} = z_{Ra} \oplus z_{Ca} \oplus (z_{Rb} \otimes z_L \otimes z_{Cb}) \tag{27}$$

The homomorphism $Z_1 \leftrightarrow Y_1$ (indicated by the –1 exponent) can be used to allow writing the above using only the simpler $\oplus$ operator. For example, (27) can be written as:

$$z_{XIV} = z_{Ra} \oplus z_{Ca} \oplus (y_{Rb} \oplus y_L \oplus y_{Cb})^{-1} \tag{28}$$

A general definition of a dual, e.g., pg. 9 in [7], views each topology of Fig. 6 as an undirected connected graph. The lumped elements form 'edges' of the graph that divide a plane into 'faces'. An edge is added to the graph to represent the source driving the network. The graph of the network's dual has one node in each original face and one edge crossing each original edge. A dual exists if and only if the original graph is planar, i.e., no two edges of the original graph cross, theorem 3-15 in [7]. All graphs that have fewer than five nodes or nine edges are planar, theorem 3-17 in [7].

There is no dual topology shown for topology XXXIII, which resembles the Wheatstone bridge. The rules for forming a dual topology, above, fail for this topology as it cannot be formed using only $\oplus$ and $\otimes$. Instead, inspection of the transfer function reveals that the dual network is formed by swapping elements 1 with 5 and 2 with 4, as well as swapping inductors and capacitors, inverting resistances, concluding by inverting the transfer function. The topology itself remains unchanged. This is confirmed by forming a dual using the method from [7] as described in the previous paragraph. Thus, this topology is its own dual.

XII. APPLICATION EXAMPLE

A method to measure the dielectric constant of a planar substrate [15] relies on precise determination of the resonant frequencies of a dual-mode (i.e., two-conductor) resonator. The difference between the even and odd mode resonant frequencies are used to determine the normal (to the substrate surface) and tangential dielectric constants. The mapping between the resonant frequencies and the desired dielectric constants is determined by ultra-precise EM analysis. Using resonators many wavelengths long, the resulting large number of resonances allows broadband characterization of the substrate dielectric constant. However, when evaluating only the center frequency of each resonance, no other information can be extracted.

Fig. 10 shows one of these resonances ('base' data). This is the eighth even-mode resonance of a long dual mode resonator on a Rogers RO3010 substrate. The fit that resulted for XXXIII-35, CR577 is shown. Note that there are two

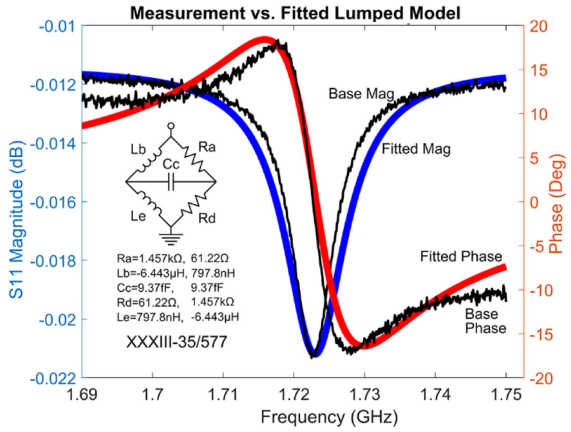

FIGURE 10. One of about 60 networks fitted to one of dozens of resonances used to characterize the dielectric constant of a substrate. The value of the fitted elements can be used to characterize substrate dielectric and magnetic constants and both conductor and dielectric loss.

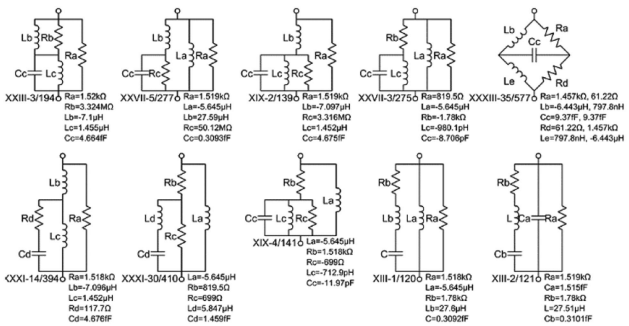

FIGURE 11. The best 10 networks fitted to the measured data of Fig. 10. All provide nearly identical results. Even though most have negative valued elements, all provide passive, positive-real admittances.

solutions for this component, each giving identical results. In this case, this is due to the component's horizontal axis of symmetry. The several thousand measured data points framing the resonance are helpful for reducing fitting error.

After fitting all available networks to this data, about 60 networks had low, nearly identical fitting errors. The top ten are shown in Fig. 11. The fitting plots for all 60 components are visually identical. Even though most (but not all) of the components have a negative-valued element, all but six are passive, i.e., positive-real.

This large resonator is a distributed circuit. Such circuits can require excessively large lumped-models. Critical to finding a simple model in this case is shifting the measured data reference plane (by adding a negative-length transmission line) so that the phase slope above and below resonance is close to zero and removing, at least over a small band, its distributed nature.

In application, one would characterize the mapping between the component element values and the substrate dielectric constants, magnetic constants, dielectric loss, and conductor loss. The network would be fitted to each resonance

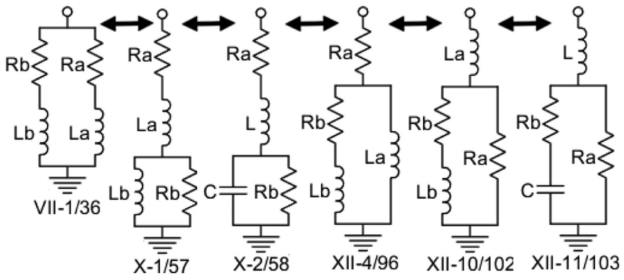

FIGURE 12. Six equivalent networks. Network X-2, CR58, is often used to synthesize a lumped model for Vector Fitting results, however, any of these six four-element networks may be used. Symbolic equations for converting between each of these networks are stored in each network's CRCat data structure.

with the resulting values used to completely electrically characterize the substrate at the frequency of each resonance.

XIII. FUTURE WORK

Vector Fitting yields the transfer function as a sum of partial fractions. Some of these terms represent a pair of complex conjugate poles in the form of a small rational polynomial with a polynomial signature of '11-111' (when dealing with admittance). For a time-domain analysis, an RLC network, X-2, CR58, in Fig. 12, may be used to represent each conjugate pole pair [16]. A quick exploration of the 623 networks in CRCat shows that there are five additional four-element networks, all illustrated in Fig. 12, that are equivalent to X-2. It might seem odd that a network with two inductors, e.g., VII-1, CR36, can represent a conjugate pair of poles. This is possible when one of the two inductors is endowed with a negative value. While negative elements are non-physical, they are easily realized in numerical models. Provided all element values are selected based on the conversion equations stored in the network data structure, all six of these networks have identical admittance at all frequencies.

There are also 10 five-element degenerate networks that have the same signature and simplify to any of the six four-element networks. It might be useful in some situations to facilitate the reverse process, taking one of the equivalent networks and increasing its complexity. This possibility has yet to be explored.

Another open item is that, given measured data, CRCat presently evaluates fits for all networks that have synthesis equations. The algorithm can be made more efficient by evaluating a fit for only one member of any equivalence set as all other members will have near identical fits. However, if this is done, then the user needs to be able to easily and quickly evaluate which member of the equivalence set is to be used.

There is one three-element network, IV-5, CR25, that also has a polynomial signature of '11-111', however it cannot represent a pair of conjugate poles.

The usual net result of Vector Fitting is to expand a rational polynomial transfer function into partial fractions and build a lumped model of, typically, simple lumped networks all connected in parallel. This is done with no need to explicitly evaluate the full rational polynomial.

Now, with numerical precision limits essentially removed, we explicitly evaluate the full rational polynomial transfer function. This enables new strategies. For example, we could perform a partial fractions expansion directly on the fitted admittance rational polynomial yielding a Vector Fitting-style model consisting of a group of simple lumped networks all connected in parallel.

A more advanced approach would be to evaluate the poles of the transfer function, select a few of them, perform a partial fractions-like extraction of the selected poles from the original transfer function splitting the transfer function into the sum of two smaller rational polynomials. One would be simple enough to find a network in CRCat that fits, and the other would be the remainder. Repeat the above procedure until the remainder polynomial is reduced to zero.

The above procedure can be modified by inverting the remainder polynomial. When extracting from a remainder polynomial that represents admittance, connect the extracted component in parallel. When extracting from an impedance polynomial, connect the extracted component in series. In this way, we are taking advantage of the homomorphism $Z_1 \leftrightarrow Y_1$ (Section VI) to use the simpler operation, $\oplus$, to synthesize any network constructable using $\oplus$ and $\otimes$.

In another option, rather than seeking an optimal model, one could seek to synthesize a specific model constructed from a specific sequence of series and shunt component extractions of specific networks. For example, one could seek to populate a specific model for a spiral inductor based on measured data. MATLAB routines for performing extractions of this nature directly from numerical data have been written and are available in the software download that accompanies this paper. Finding an optimal extraction from the fitted rational polynomial has not been investigated and will likely require significant effort for potentially major return. Perhaps this is an application for artificial intelligence.

Multi-port structures can be formed from multiple two-terminal networks as detailed in [12]. Given N-port measured data, generation of a N-port Pi-model requires models based on the measured data with various ports terminated in short circuits. Generation of N-port Tee-models requires data with ports terminated in open circuits. Note that for more than two ports, Tee-models require ideal transformers, [12]. Typically, both models should be generated for a given data set to determine which one provides better results.

When optimization must be used, we can reduce the number of optimization variables. If a desired model has N elements, add a custom model to CRCat by specifying variable names for the elements and providing a net list for their connection. CRCat is then tasked to incorporate this model into its library. In doing so, it will attempt to derive synthesis equations so the element values can be determined directly from the fitted rational polynomial coefficients. If there is no solution for the synthesis equations, select one or more of the elements to remain unsolved. The synthesis equations that result will now have those unsolved element values as

unknowns in the synthesis equations. In this way, at least four, and likely more element values will be synthesized and represented as functions of the unsolved element values. Then one would invoke optimization to optimize the remaining element values.

The reason MATLAB cannot derive synthesis equations for all minimal networks might be because of limits in its symbolic solver. Another possibility is related to the fact that the solution might require a general algebraic solution to the quintic equation. It has been proven that such a solution does not exist [17].

The rich palette of network relationships revealed in this work can be useful in filter synthesis. Early work in this area [14] found several useful equivalences that have had substantial impact on filter synthesis. In this work, we list all known equivalent, degenerate, regenerate, and compound transforms between two-terminal lumped networks of five or fewer elements. All transform equations for the thousands of relationships found have been derived and are available in CRCat. Making this information available to the designer in an easily digested form remains an open work item.

XIV. CONCLUSION

For the first time, a catalog, CRCat, of all possible lumped two-terminal RLC networks composed of five or fewer elements is described. Extensive information about each network has been evaluated and included in CRCat. A MATLAB script is now available [5] that automatically derives and stores symbolic equations for each transfer response in terms of a rational polynomial, symbolic equations for poles and zeros, and symbolic synthesis equations (given a rational polynomial with numerical coefficients, determine the RLC values that yield that rational polynomial). Thousands of transform relations between pairs of networks have been identified with transform equations provided for most of them. A MATLAB script for a direct least-squares fit to find a best fitting numerical rational polynomial from measured data is provided. The script uses MATLAB variable precision arithmetic to enable solution of 1200 rational polynomial terms using arithmetic with a numerical mantissa size of 700 digits, for example. The least-squares fit is unique in that it provides only rational polynomials that are perfectly causal. The resulting catalog, CRCat, is freely available [5] as a download associated with this paper. Finally, a proposal for casting lumped element network analysis and extraction in the framework of group theory has been presented.

REFERENCES

[1] C. Sanathanan and J. Koerner, "Transfer function synthesis as a ratio of two complex polynomials," *IEEE Trans. Autom. Control*, vol. AC-8, no. 1, pp. 56–58, Jan. 1963, doi: 10.1109/TAC.1963.1105517.

[2] B. Gustavsen and A. Semlyen, "Rational approximation of frequency domain responses by vector fitting," *IEEE Trans. Power Del.*, vol. 14, no. 3, pp. 1052–1061, Jul. 1999, doi: 10.1109/61.772353.

[3] P. Triverio, "Vector fitting," 2019, *arXiv:1908.08977*.

[4] J. C. Rautio, "Synthesis of compact lumped models from electromagnetic analysis results," *IEEE Trans. Microw. Theory Techn.*, vol. 55, no. 12, pp. 2548–2554, Dec. 2007, doi: 10.1109/TMTT.2007.909141.

[5] 2025. [Online]. Available: https://github.com/Sonnet-Software/CRCat

[6] (n.d.). [Online]. Available: https://www.eeeguide.com/positive-real-function/

[7] A. Morelli, "Synthesis of electrical and mechanical networks of restricted complexity," Ph.D. dissertation, Dept. Eng., Univ. Cambridge, Cambridge, U.K., 2019.

[8] *Sonnet Software User's Manual*, 18th ed. Syracuse, NY, USA: Sonnet Software, 2023.

[9] J. C. Rautio, *Method of Moments Analysis of Structures Embedded in Shielded Layered Media*. Amazon, 2020, ISBN-13: 979–8714970481.

[10] J.-M. Collantes et al., "Pole-zero identification: Unveiling the critical dynamics of microwave circuits beyond stability analysis," *IEEE Microw. Mag.*, vol. 20, no. 7, pp. 36–54, Jul. 2019, doi: 10.1109/MMM.2019.2909516.

[11] K. R. McLean, "Groups of rational functions," 2007. [Online]. Available: https://www.jstor.org/stable/40378343

[12] J. C. Rautio, "N-Port T-networks and topologically symmetric circuit theory," *IEEE Trans. Microw. Theory Techn.*, vol. 58, no. 4, pp. 705–709, Apr. 2010, doi: 10.1109/TMTT.2010.2041516.

[13] E. L. Ladenheim, "A synthesis of biquadratic impedances," M.S. thesis, Polytechnic Inst., Brooklyn, New York, NY, USA, 1948.

[14] A. I. Zverev, *Handbook of Filter Synthesis, Library of Congress catalog card number: 67-17352*, Wiley, New York, NY, USA, 1967, pp. 522–527.

[15] J. C. Rautio, R. L. Carlson, B. J. Rautio, and S. Arvas, "Shielded dual-mode microstrip resonator measurement of uniaxial anisotropy," *IEEE Trans. Microw. Theory Techn.*, vol. 59, no. 3, pp. 748–754, Mar. 2011, doi: 10.1109/TMTT.2010.2103211.

[16] G. Antonini, "SPICE equivalent circuits of frequency-domain responses," *IEEE Trans. Electromagn. Compat.*, vol. 45, no. 3, pp. 502–512, Aug. 2003, doi: 10.1109/TEMC.2003.815528.

[17] (n.d.). [Online]. Available: https://en.wikipedia.org/wiki/Abel-Ruffini_theorem

JAMES C. RAUTIO (Life Fellow, IEEE) received the B.S.E.E. degree from Cornell University, Ithaca, NY, USA, in 1978, the M.S. degree in systems engineering from the University of Pennsylvania, Philadelphia, PA, USA, in 1981, and the Ph.D. degree, under Dr. Roger Harrington, in electrical engineering from Syracuse University, Syracuse, NY, USA, in 1986.

From 1978 to 1986, he was with General Electric, initially with the Valley Forge Space Division, then with the Syracuse Electronics Laboratory. During this time, he developed microwave design and measurement software and designed microwave circuits on alumina and on GaAs. From 1986 to 1988, he was a Visiting Professor with Syracuse University and Cornell University. In 1988, he took Sonnet Software, North Syracuse, NY, full time, a company he had founded in 1983. In 1995, Sonnet Software was listed on the Inc. 500 list of the fastest growing privately held U.S. companies, the only microwave software company ever to be so listed. Today, Sonnet Software is the leading vendor of high accuracy three-dimensional planar high-frequency electromagnetic analysis software.

He was the recipient of the 2001 IEEE Microwave Theory and Techniques Society (IEEE MTT-S) Microwave Application Award, 2014 MTT Distinguished Service Award, and the 2019 MTT Career Award. He was appointed MTT Distinguished Microwave Lecturer from 2005 to 2007 lecturing on the life of James Clerk Maxwell.